PNAS RESEARCH ARTICLE | MEDICAL SCIENCES

A hypothalamic pathway for Augmentor α–controlled body weight regulation

Mansoor Ahmed[a,1], Navjot Kaur[b], Qianni Cheng[a], Marya Shanabrough[c], Evgenii O. Tretiakov[d], Tibor Harkany[d,e], Tamas L. Horvath[b,c], and Joseph Schlessinger[a,1]

Contributed by Joseph Schlessinger; received January 10, 2022; accepted March 15, 2022; reviewed by Umut Ozcan and Emmanuel Van Obberghen

Augmentor α and β (Augα and Augβ) are newly discovered ligands of the receptor tyrosine kinases Alk and Ltk. Augα functions as a dimeric ligand that binds with high affinity and specificity to Alk and Ltk. However, a monomeric Augα fragment and monomeric Augβ also bind to Alk and potently stimulate cellular responses. While previous studies demonstrated that oncogenic Alk mutants function as important drivers of a variety of human cancers, the physiological roles of Augα and Augβ are poorly understood. Here, we investigate the physiological roles of Augα and Augβ by exploring mice deficient in each or both Aug ligands. Analysis of mutant mice showed that both Augα single knockout and double knockout of Augα and Augβ exhibit a similar thinness phenotype and resistance to diet-induced obesity. In the Augα-knockout mice, the leanness phenotype is coupled to increased physical activity. By contrast, Augβ-knockout mice showed similar weight curves as the littermate controls. Experiments are presented demonstrating that Augα is robustly expressed and metabolically regulated in agouti-related peptide (AgRP) neurons, cells that control whole-body energy homeostasis in part via their projections to the paraventricular nucleus (PVN). Moreover, both Alk and melanocortin receptor-4 are expressed in discrete neuronal populations in the PVN and are regulated by projections containing Augα and AgRP, respectively, demonstrating that two distinct mechanisms that regulate pigmentation operate in the hypothalamus to control body weight. These experiments show that Alk-driven cancers were co-opted from a neuronal pathway in control of body weight, offering therapeutic opportunities for metabolic diseases and cancer.

cell signaling | phosphorylation | metabolism | surface receptors | energy expenditure

Receptor tyrosine kinases (RTKs) represent an important family of cell surface receptors that regulate numerous essential cellular responses during embryonic development and in the homeostasis of adult organisms (1). Alk was originally discovered as an oncogenic RTK fusion protein endowed with constitutively activated tyrosine kinase activity generated by chromosomal translocation in a subset of anaplastic large cell lymphoma (2). At least 20 distinct partners of oncogenic Alk fusion proteins generated by chromosomal translocations as well as germline and somatic Alk mutations were identified as key drivers of a variety of cancers, including large B cell lymphomas, inflammatory myofibroblast tumors, and pediatric neuroblastoma (3–6). As physiological ligands of full-size Alk and of a second family member designated Ltk were not known for two decades, the two RTKs were classified as "orphan receptors".

In 2014, Zhang et al. identified two secreted proteins of unknown function designated FAM150A and FAM150B as ligands that bind specifically to Ltk and stimulate Ltk activation (7). It was subsequently demonstrated that these proteins, also designated Augmentor α (Augα; or ALKAL2) and Augmentor β (Augβ; or ALKAL1), function as specific and potent ligands of Alk (8, 9). Biochemical characterization showed that Augα functions as a dimeric ligand of both Alk and Ltk, and that a conserved cysteine residue located in the N-terminal variable region of primate Augα is responsible for mediating Augα dimerization via formation of a disulfide bond between two Augα molecules (10). We have also demonstrated that a monomeric fragment composed of the conserved C-terminal region of Augα efficiently stimulates activation and cell signaling in Alk- or Ltk-expressing cultured cells (10). Recent biochemical and structural characterization demonstrated that Augβ functions as a monomeric activating ligand of Alk and Ltk, demonstrating and revealing a mechanism of how dimeric or monomeric Aug proteins stimulate Alk dimerization, activation, and cellular signaling (11).

The first insight concerning the biological role of Aug proteins emerged from genetic studies of zebrafish pigment development. These studies demonstrated that zebrafish Aug homologs and Alk homologs are components of a cellular signaling pathway controlling neural crest–derived pigment cell development in zebrafish (12, 13). It also

Significance

The receptor tyrosine kinase Alk was originally discovered as an oncogenic fusion protein generated in anaplastic large cell lymphoma. A variety of oncogenic Alk fusion proteins were subsequently identified as key drivers of subsets of different cancers, including non-small cell lung cancer patients, large B cell lymphomas, and inflammatory myofibroblast tumors. In addition, activating oncogenic somatic mutations were identified in populations of pediatric neuroblastoma patients. Crizotininb, lorlatinib, and other drugs that inhibit the tyrosine kinase activity of Alk were successfully applied for the treatment of patients harboring oncogenic Alk mutants. In this report, we present experiments demonstrating that the physiological ligands of Alk function in the hypothalamus to control body weight, offering new therapeutic treatments for metabolic diseases and cancer.

Author contributions: M.A., N.K., Q.C., T.L.H., and J.S. designed research; M.A., N.K., Q.C., M.S., E.O.T., and T.H. performed research; M.A., N.K., E.O.T., T.H., T.L.H., and J.S. analyzed data; and M.A., N.K., T.H., T.L.H., and J.S. wrote the paper.

Reviewers: U.O., Children's Hospital/Harvard Medical School; and E.V.O., INSERM Unit 145.

The authors declare no competing interest.

[1]To whom correspondence may be addressed. Email: mansoor.ahmed@yale.edu or joseph.schlessinger@yale.edu.

This article contains supporting information online at http://www.pnas.org/lookup/suppl/doi:10.1073/pnas.2200476119/-/DCSupplemental.

Published April 11, 2022.

provided in vivo evidence for a functional ligand/receptor link between Aug and Alk homologs during neural crest development in zebrafish.

Results

Augα Is Expressed in Agouti-Related Peptide (AgRP)–Positive Neurons within the Arcuate Nucleus (ARC) in the Hypothalamus. To elucidate the physiological roles of Augα and Augβ in mammals, we generated individual knockout mice and double knockout mice of Augα and Augβ. Augα-knockout mice were generated by replacing exons 1 to 4 with a green fluorescent protein (GFP) expression cassette to enable analysis of the expression pattern of endogenous Augα protein in both tissues and cells. Similarly, Augβ-knockout mice were generated by replacing exon 1 with a GFP expression cassette. Double knockout mice were generated by crossing Augα- and Augβ-deficient mice (*SI Appendix*, Fig. S1 *A*–*C*). We also generated another line of knockout mice by replacing Augα with a LacZ cassette (i.e., AugαLacZ/+ and AugαLacZ/LacZ mice; *SI Appendix*, Fig. S1 *D* and *E*).

Using Augα-Gfp/+ and Augβ-Gfp/+ mice, we next analyzed the expression of Augα and Augβ primarily within the brain. Visualization of Augα-Gfp/+ mice by immunofluorescence microscopy revealed strong expression in the hypothalamus (Fig. 1*A*). To determine whether loss of Augα may cause changes in cytoarchitecture and in the localization of neuronal cell populations expressing Augα, we generated and similarly analyzed Augα-Gfp/Gfp–knockout mice. No obvious defects were observed in the overall brain anatomy and in the region containing cells labeled by Augα–GFP (Fig. 1*A*). The most robust expression of Augα was detected within the ARC, with weaker expression in the paraventricular nucleus (PVN), dorsomedial nucleus (DMH), and suprachiasmatic nucleus (SCN; Fig. 1 *A* and *B*).

Next, we determined the cell types expressing Augα within the ARC nucleus. The ARC nucleus contains two major neuronal cell populations that control energy metabolism, including hunger-promoting AgRP neurons and satiety-promoting proopiomelanocortin (POMC) neurons (14, 15). To determine the specific cells within the ARC that express Augα, we immunolabeled postnatal day 60 (P60) coronal sections of Augα-Gfp/+ mice with anti-neuropeptide Y (NPY) antibody, which also labels AgRP neurons (*SI Appendix*, Fig. S2*A*), and with an anti-POMC antibody that labels POMC neurons (*SI Appendix*, Fig. S2*B*). This experiment showed increased coexpression of NPY-positive neurons with GFP-labeled neurons, suggesting endogenous expression of Augα in AgRP neurons within the ARC. Moreover, published single-cell RNA-sequencing data (16) revealed high expression of Augα (Fam150B) within AgRP neurons among 18 neuronal cell populations (*SI Appendix*, Fig. S2 *C* and *D*). To further establish colocalization of Augα–Gfp within the ARC neuronal populations, we genetically labeled Augα–Gfp-expressing cells within the ARC nucleus using AgRP-Cre; Ai14-tdT mice that label all AgRP-expressing neurons (in red) and POMC-Cre; Ai14-tdT mice that label all POMC-expressing neurons (in red; Fig. 1 *C* and *D*). The Augα–Gfp neurons within the ARC showed strong colocalization with the AgRP-expressing neurons and minimal colocalization with POMC neurons. It is noteworthy that we were not able to detect Augβ expression in the brain, which is consistent with open-label RNA-sequencing data (17), which also did not reveal Augβ mRNA expression in the brain (*SI Appendix*, Fig. S2*E*). Taken together these experiments show a particularly high expression of Augα in AgRP neurons in the ARC nucleus of the hypothalamus.

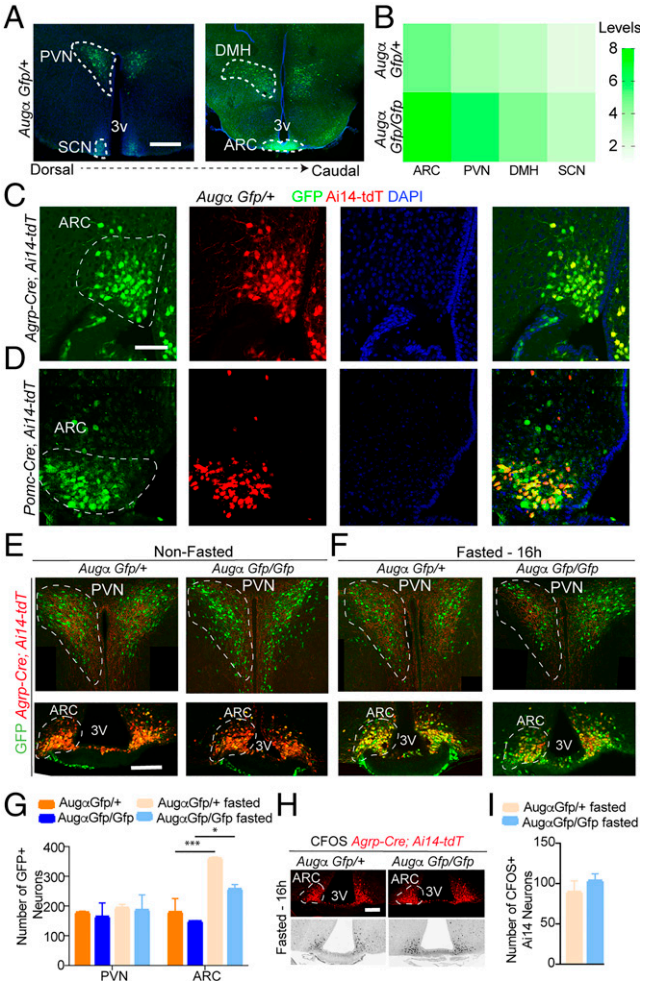

Fig. 1. Augα is predominantly expressed in AgRP neurons within the ARC, and its expression is increased upon fasting. (*A*) Expression of Gfp within the hypothalamus in the Augα-Gfp/+ animals at P90. (Scale bar, 500 μm.) (*B*) Heat map showing the level of Gfp expression within the Augα-Gfp/+ and Augα-Gfp/Gfp mice at P90 ($n = 3$). (*C* and *D*) Coronal sections of Augα-Gfp/+; AgRP-Cre; Ai14-tdT (*C*) and Augα-Gfp/+; POMC-Cre; Ai14-tdT (*D*) animals at P60 showing predominant colocalization of Augα and AgRP. (Scale bar, 40 μm.) (*E* and *F*) Expression of GFP (Augα) and red fluorescent protein (AgRP) within the ARC and PVN of the Augα-Gfp/+; AgRP-Cre; Ai14-tdT and Augα-Gfp/Gfp; AgRP-Cre; Ai14-tdT mice under normal conditions (*E*) and under 16 h of food deprivation. 3V is 3rd ventricle (*F*). (Scale bar, 40 μm.) (*G*) Quantifications of Aug–Gfp expression within the ARC and PVN from *E* and *F*. Data in the figure are presented as mean ± SEM. A two-way ANOVA with Bonferroni's multiple comparisons test was applied; $^{***}P < 0.001$, $^{**}P < 0.01$ ($n = 4$). (*H*) Expression of c-Fos within the ARC nuclei of the Augα-Gfp/+; AgRP-Cre; Ai14-tdT and Augα-Gfp/Gfp; AgRP-Cre; Ai14-tdT mice after 16 h of food deprivation. (Scale bar, 20 μm.) (*I*) Quantification of c-Fos in Ai14-tdT–positive cells from *H*. A two-way ANOVA with Bonferroni's multiple comparisons test was applied ($n = 3$).

Fasting Stimulates Augα Expression in AgRP Neurons. AgRP neurons located within the ARC of the hypothalamus are critical for regulating food intake and energy homeostasis (18). In response to fasting, AgRP neurons show increased expression of various orexigenic molecules, including AgRP peptide, which regulates neurons in the PVN (19). To determine whether Augα expression within the ARC nucleus is involved in control of hunger and satiety, we performed a 16-h food starvation study on the Augα-Gfp/+; AgRP-Cre; Ai14-tdT and Augα-Gfp/Gfp; AgRP-Cre; Ai14-tdT animals. We observed that Augα is metabolically stimulated upon fasting within AgRP

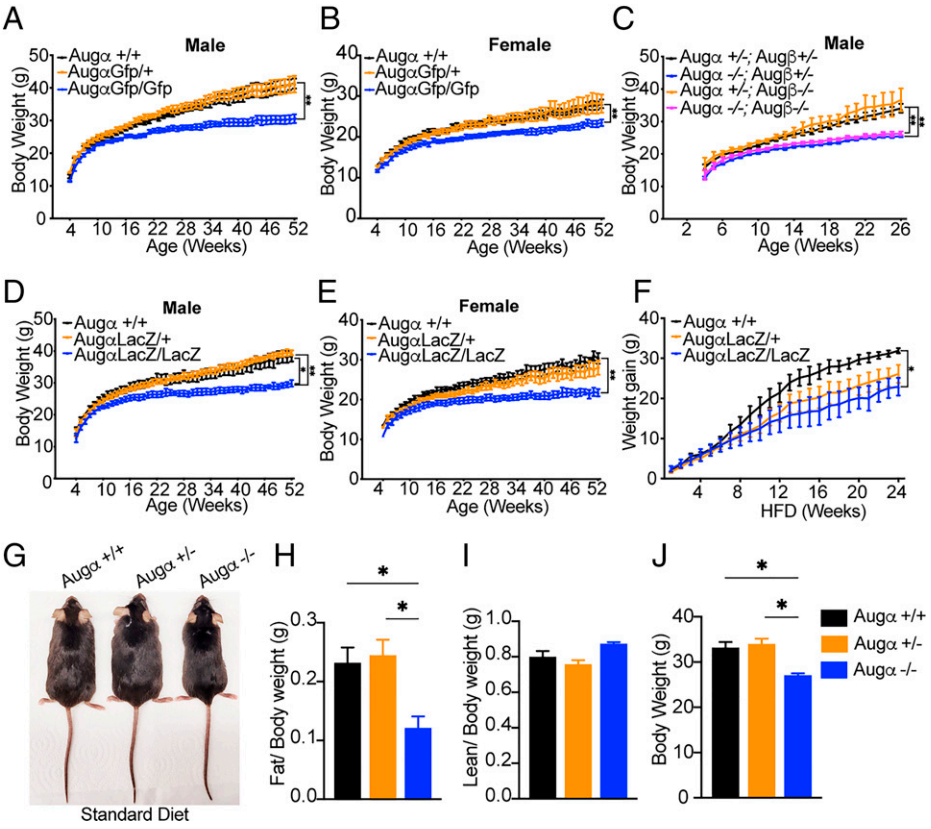

Fig. 2. Augα-knockout mice are thin. (*A* and *B*) Body weight kinetics of Augα$^{+/+}$; Augα-Gfp/+; Augα-Gfp/Gfp littermate male (*A*) and female (*B*) mice fed on a standard diet ($n \geq 6$). (*C*) Body weight kinetics of Augα-Gfp and Augβ-Gfp single and double knockout mice and littermate double heterozygous male mice on a normal diet ($n \geq 5$). (*D* and *E*) Body weight in the Augα$^{+/+}$; Augα-Lacz/+; Augα-Lacz/Lacz littermate male (*D*) and female (*E*) mice fed on a standard diet; $n \geq 4$ in *A*, and $n \geq 5$ in *B*. (*F*) Body weight gain from male and female Augα-knockout, heterozygous, and wild-type littermate mice on a HFD ($n \geq 5$). (*G*) Representative image showing the gross morphology of 36-wk–old Augα-knockout, heterozygous, and wild-type mice on a standard diet. (*H*–*J*) MRI analysis of fat (*H*), lean mass (*I*), and body weight (*J*) ($n \geq 5$). Data in the figure are presented as mean ± SEM. A one- or two-way ANOVA with Bonferroni's multiple comparisons test was applied; *$P < 0.05$, **$P < 0.01$.

neurons, while its expression within PVN remains unchanged (Fig. 1 *E*–*G* and *SI Appendix*, Fig. S3). RNA seq (17) data also showed similarly increased expression of Augα in AgRP neurons upon fasting versus refeeding (*SI Appendix*, Fig. S2*E*). However, the increased expression of Augα did not affect AgRP neuron activation, as shown by c-Fos immunostaining in Augα-Gfp/Gfp versus Augα-Gfp/+ animals (Fig. 1 *H* and *I*), suggesting that Augα may act downstream from AgRP signaling.

To determine whether Augα governs any of the metabolic phenotype during fasting, we performed fasting and refeeding experiments on Augα-knockout and wild-type littermate mice in metabolic cages. Single animals were housed for 4 d in the metabolic cage, and at the end of day four, the mice were food deprived for 16 h and then allowed to feed for the next 24 h. During food deprivation, significantly higher energy expenditure and respiratory exchange rate (RER) of Augα-deficient mice were detected due to increased CO_2 production during the dark phases, indicating a preference for carbohydrate consumption over lipids with activity trending higher (*SI Appendix*, Fig. S4). A significant increase in water intake was also detected in Augα-deficient mice during the dark phase of the fasting period (*SI Appendix*, Fig. S4*E*). However, upon refeeding, a small but significant decrease in both food and water intake was observed in Augα-deficient mice as compared to their wild-type littermates (*SI Appendix*, Fig. S5). Taken together, the results showed that Augα expression increases upon fasting similar to the expression of other orexigenic genes, including AgRP and Npy. These results link Augα to the metabolic circuit of AgRP-controlled energy homeostasis (20).

Augα-Knockout Mice Are Thin. To determine the effect of Augα deficiency on animal physiology, we assessed the weight and body composition of the Augα-knockout and littermate control mice. The mice were born according to the Mendelian ratio. We observed that both Augα male and female knockout mice, derived from both Gfp- and LacZ-knockin mouse lines, gained less weight with age than wild-type littermate or heterozygous mice on standard chow diet. Differences in body weights were noticed from the age of 4 wk onward. Moreover, from the age of 14 wk onward, Augα-knockout animals (male and female) were significantly leaner than Augα heterozygous or wild-type animals. There was no significant weight difference between heterozygous and wild-type mice (Fig. 2 *A*, *B*, *D*, and *E*). The Augα and Augβ double knockout mice and Augα single knockout mice showed similar age-dependent weight differences compared to the double heterozygous mice. In contrast, the Augβ-knockout mice, which carry one Augα allele, showed no weight difference compared to double heterozygous littermates. These results demonstrate that Augα deficiency is critical for thinness, while Augβ deficiency does not cause thinness (Fig. 2*C*). In addition, Augα-knockout mice gained significantly less weight than littermate controls when the mice were fed a high-fat diet (HFD), suggesting that Augα deficiency provides resistance against HFD-induced weight gain (Fig. 2*F*). Inspection of the gross morphology of the animals revealed a substantial reduction in the circumference of the animals but no change in their length, indicating that the differences seen in the weights of males and females are not due to change in body length (Fig. 2*G*). We next analyzed the body composition

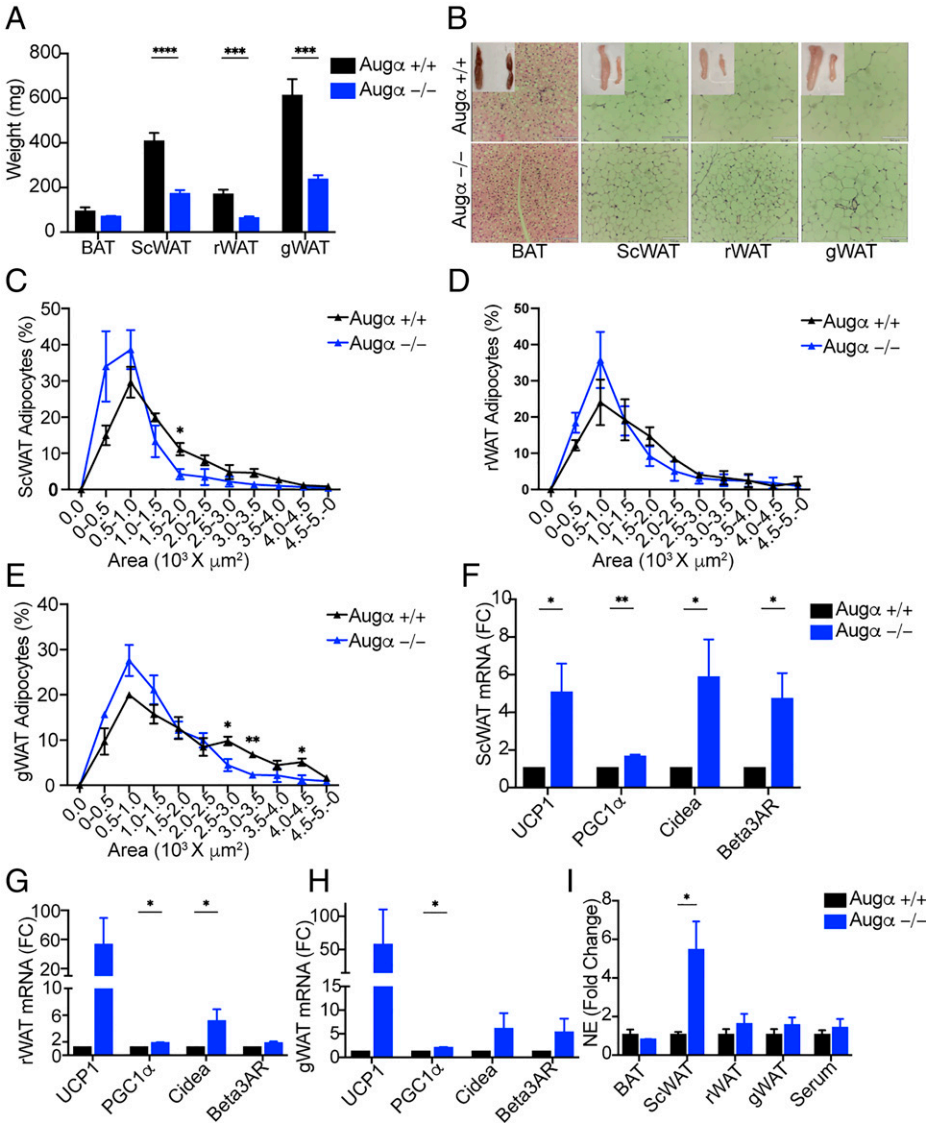

Fig. 3. Augα-knockout mice exhibit decreased adiposity. (*A*) Bar plot showing the weights of fat mass from BAT, scWAT, rWAT, and gWAT; $n \geq 8$. (*B*) Representative H&E image of BAT, scWAT, rWAT, and gWAT showing decreased size of the adipocytes in Augα-knockout versus wild-type mice. (Scale bar, 120 μm.) (*C–E*) Line graph showing quantification of adipocyte area from scWAT (*C*), rWAT (*D*), and gWAT (*E*); $n = 3$. (*F–H*) qRT-PCR quantification of fatty acid oxidation and thermogenesis genes (*UCP1*, *PCG1a*, *Cidea*, and *Beta3AR*) in scWAT (*F*), rWAT (*G*), and gWAT (*H*); $n \geq 9$. (*I*) Quantification of NE level from BAT, scWAT, rWAT, gWAT, and sera; $n \geq 8$. Data in the figure are presented as mean ± SEM. A two-tailed unpaired Student's *t* test was applied; $^{*}P < 0.05$, $^{**}P < 0.01$, $^{***}P < 0.001$, $^{****}P < 0.0001$.

of adult Augα-knockout mice and their littermate wild-type as well as heterozygous controls by magnetic resonance imaging (MRI). This analysis revealed that Augα-knockout mice have significantly less overall body fat and more lean mass than wild-type and heterozygous littermate mice with respect to their overall body weight (Fig. 2 *H–J*).

Furthermore, to determine the contributions of each of the fat deposits, fat from subcutaneous white adipose tissue (scWAT), retroperitoneal WAT (rWAT), and gonadal WAT (gWAT) as well as brown adipose tissue (BAT) from Augα-knockout and wild-type animals was isolated. The results presented in Fig. 3*A* revealed significantly reduced weight of scWAT, rWAT, and gWAT in Augα-knockout mice. Overall gross anatomy revealed reduction in the size of the adipose tissue depots in the Augα-knockout mice, which were further analyzed by hematoxylin and eosin (H&E) staining to assess fat composition and adiposity. Overall, lower percentages of large adipocytes were detected in Augα-knockout mice than in their littermate controls; conversely, a higher percentage of small adipocytes was detected in Augα-knockout mice (Fig. 3 *B–E*). To gain insight into the mechanism of reduced fat deposition in the adipocytes of Augα-knockout mice, qRT-PCR analysis was carried out for genes involved in the control of thermogenesis and fat oxidation. The experiment presented in Fig. 3 *F–H* reveals increased expression levels of mitochondrial brown fat uncoupling protein 1 (UCP1), peroxisome proliferator–activated receptor coactivator 1α (PGC1α), cell death activator (*CIDEA-A*), and β3 adrenergic receptor (β3AR) in WAT depots, suggesting some browning of WAT. To determine a potential link between decreased Augα expression in brain and increased browning of WAT, we next analyzed the levels of norepinephrine (NE) produced in adipose tissue and in the sera of Augα-knockout and control mice. This experiment revealed a strong increase of NE levels in scWAT (Fig. 3*I*). It was previously demonstrated that hypothalamic PVN neurons regulate NE production within adipocytes through a cascade of neuronal connections, resulting in enhancement of thermogenesis and fat oxidation (21). While our experiments reveal changes in adipose tissue depots in Augα-

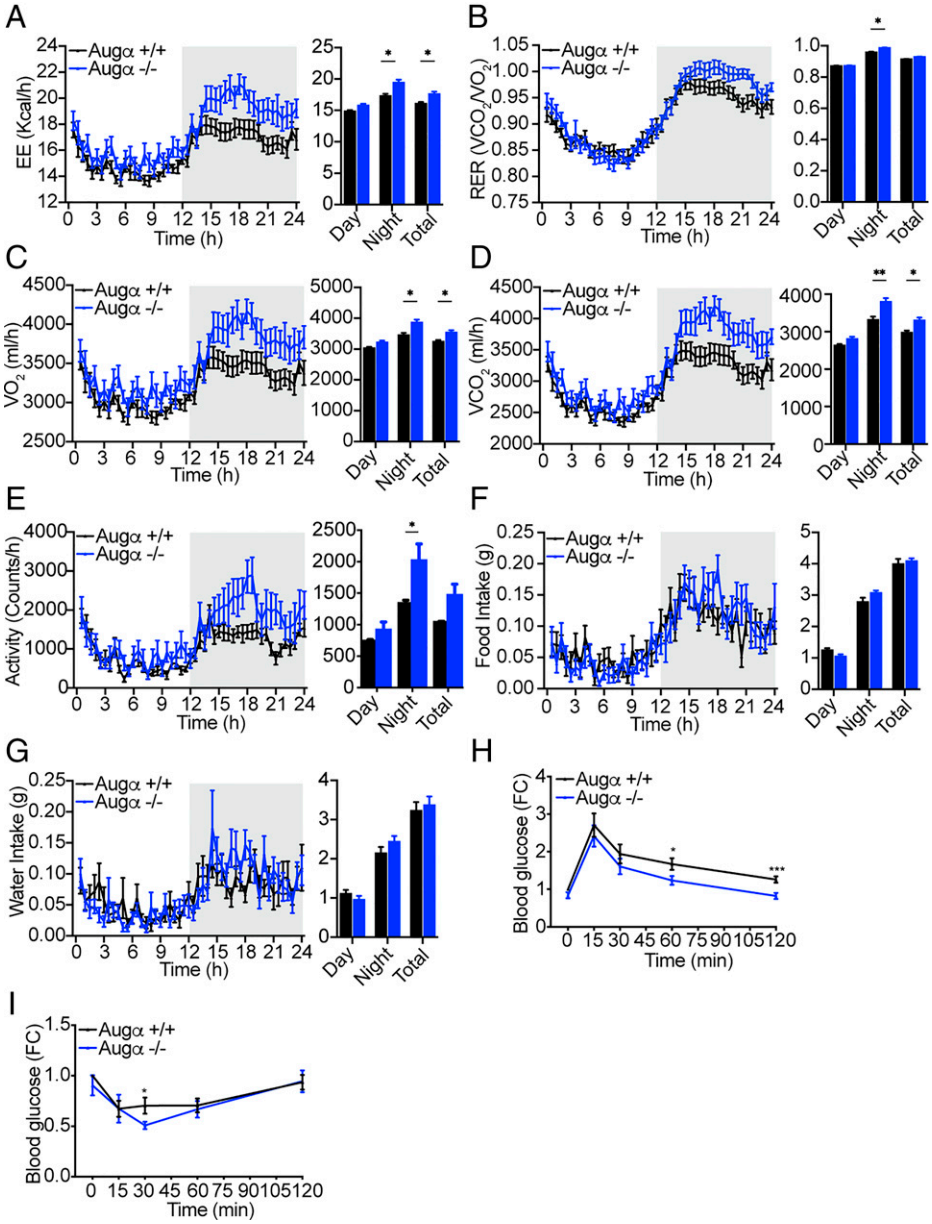

Fig. 4. Augα-knockout mice show increased energy expenditure and glucose tolerance. (*A*–*G*) Line plots showing the kinetics of energy expenditure (EE) (*A*), RER (*B*), oxygen consumption (VO_2) (*C*), CO_2 production (VCO_2) (*D*), activity (*E*), food intake (*F*), and water intake (*G*) during light (white) and dark (gray) phases; $n \geq 14$. (*H* and *I*) Line graph showing kinetics of glucose clearance (*H*) and insulin tolerance (*I*); $n \geq 12$. Data in the figure are presented as mean ± SEM. A two-tailed unpaired Student's *t* test was applied; $^{*}P < 0.05$, $^{**}P < 0.01$, $^{***}P < 0.001$.

knockout mice, these results may not represent the sole mechanism underlying the leanness of Augα-knockout mice.

Increased Energy Expenditure and Physical Activity of Augα-Knockout Mice. To approach the mechanisms contributing to the lean phenotype of the Augα-knockout mice, we compared 3- to 6-mo–old Augα-knockout mice with littermate control mice fed on a standard diet in metabolic cages for 2 d. We observed that Augα-knockout mice were slightly more active during daytime but had a significantly higher activity during the night period with two separate peaks. Coherent with this, the augmented activity was associated with higher energy expenditure and RER contributed by increased O_2 consumption and CO_2 production (Fig. 4 *A*–*E*). However, while during the night period, food and water intake tend to be increased in the lean knockout mice, this did not reach statistical significance (Fig. 4 *F* and *G*). We also assessed these animals for glucose tolerance and insulin sensitivity. The experiment presented in Fig. 4 *H*–*I* illustrates that Augα deficiency leads to improved glucose tolerance and sensitivity to insulin, consistent with increased energy expenditure and physical activity.

Taken together, the metabolic parameters suggest that the age-dependent thinness of Augα-knockout mice is the likely result of increased physical activity linked to higher energy expenditure and superior glucose clearance. However, longer and more detailed metabolic analysis may reveal the full contribution of altered food intake, possibly with behavioral changes, to the Augα-knockout mice lean phenotype.

Augα Regulates AgRP Neuronal Projection and Alk Activation in the PVN. To identify the mechanism of neuronal control of Augα-knockout mice thinness, we took a cue from our previous studies where we showed that Augα induces neurite elongation in neuroblastoma cell lines (10). To determine whether Augα

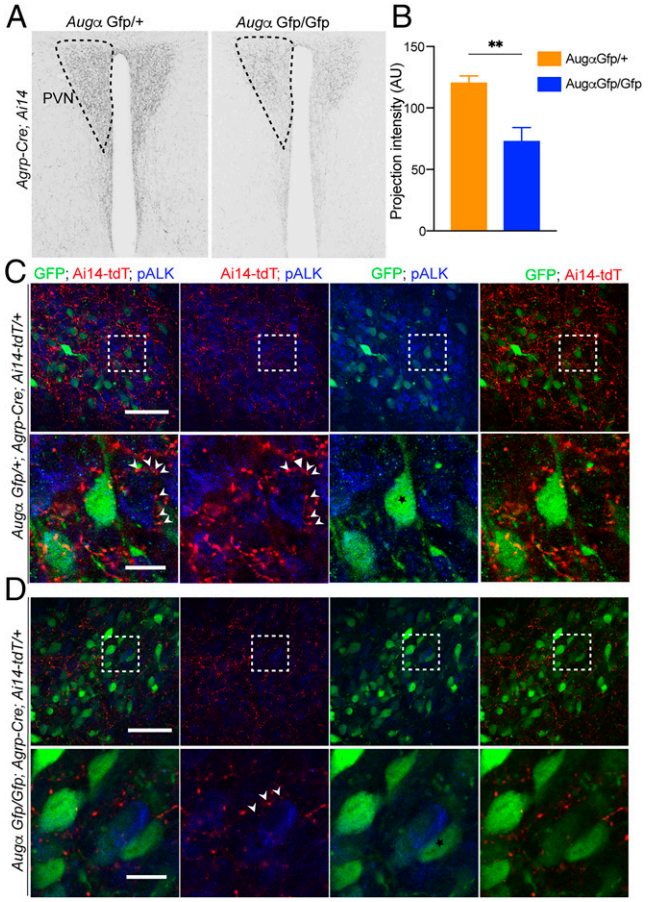

Fig. 5. Reduced AgRP projections leads to suppressed Alk phosphorylation in the PVN of Augα-deficient mice. (*A*) Image showing innervation of AgRP fibers within the PVN in Augα-Gfp/Gfp and Augα-Gfp/+ mice. (*B*) Quantification of the AgRP innervations within the PVN by measuring relative intensity. Data are presented as mean ± SEM. A two-tailed unpaired Student's *t* test was applied; $^{**}P < 0.01$ and $n \geq 6$; AU, arbitrary units. (*C* and *D*) Images showing pAlk (blue) within the PVN neurons in Augα-Gfp/+ (*C*) and Augα-Gfp/Gfp (*D*) mouse brains. The AgRP fibers from the ARC nucleus (red) are in the immediate vicinity of Alk-expressing cells (arrowheads). The Augα-expressing cells are located juxtaposed to the Alk-expressing cells (star). *Bottom*, blow up of dotted box from *Top*. Scale bars are 20μm (upper panel) and 5μm (lower panel).

can also mediate a similar response in mouse neuronal cultures, we isolated neural stem cells from a wild-type animal and stimulated them in the presence of recombinant mouse Augα protein. This experiment showed a robust increase in neurite formation, as shown in *SI Appendix*, Fig. S6*A* by staining with microtubule-associated protein-2. We next examined the possibility of whether Augα deletion may affect the arborization of AgRP neuronal projections to the PVN, a critical region that regulates energy homeostasis downstream of ARC. In this experiment serial sections of the PVN isolated from adult and P15 brains of Augα-Gfp/+; AgRP-Cre; Ai14-tdT and Augα-Gfp/Gfp; AgRP-Cre; Ai14-tdT mice were analyzed for AgRP axon arborization into the PVN. We observed that axonal projections of AgRP neurons onto PVN neurons were significantly reduced in numbers, indicating a disruption in metabolic circuitry (Fig. 5). These results suggest a potential role of Augα in the development of the metabolic circuit.

It was previously demonstrated that Alk is expressed in a subset of PVN neurons and that knockout of Alk leads to thinness (22). Additionally, in situ hybridization data of Alk from Allen Brain Atlas and experiments performed in our laboratory confirmed Alk localization in the PVN (*SI Appendix*, Fig. S6 *B* and *C*). Mechanistically, Augα binding stimulates tyrosine autophosphorylation and Alk activation, leading to stimulation of Alk-dependent intracellular signaling pathways (10). To determine if Augα expression in ARC and/or the PVN influences Alk activation within the PVN, we performed immunolabeling of Alk using antibodies that bind to the Alk extracellular domain as a measure for Alk level and phospho-Alk (pAlk)–selective antibodies as a measure of Alk activation in the brains of Augα-Gfp/+; AgRP-Cre; Ai14-tdT and Augα-Gfp/Gfp; AgRP-Cre; Ai14-tdT mice. This experiment showed that tdTomato-labeled AgRP projections are in close proximity to pAlk-expressing cell bodies, suggesting that Augα expressed in AgRP neurons may mediate activation of Alk within the PVN. Moreover, GFP-labeled Augα neurons are in the vicinity of the pAlk-expressing neurons in the PVN, revealing close proximity of endogenous Augα with Alk, consistent with Augα-induced Alk activation in these neurons. Further analysis of the Augα-Gfp/Gfp; AgRP-Cre; Ai14-tdT brains revealed that the level of pAlk is reduced in Augα-deficient mice (Fig. 5 *C* and *D* and *SI Appendix*, Fig. S6*F*), while the level of total Alk remains unaffected in the PVN of Augα-deficient mice (*SI Appendix*, Fig. S6 *D* and *E*). These results provide a mechanistic link to an earlier finding demonstrating that deletion of Alk from the PVN results in thinning of mice (22). We propose that Augα expressed in AgRP and/or the PVN stimulates Alk activation in the PVN, an area within the hypothalamus implicated in control of energy metabolism (22).

Experiments presented in this manuscript show that the Augα-activated Alk signaling pathway may operate within the hypothalamus, ARC, and PVN neurons, a region in which signaling via MC4 receptors (MC4Rs) controls an important metabolic process that regulates food intake. It was shown that binding of AgRP or melanocyte-stimulating hormone (α-MSH) to MC4R in the PVN promotes hunger or satiety, respectively, and that aberrant activation of this pathway results in severe cases of obesity (23–25). To determine whether the Augα–Alk signaling pathway is linked to or part of the α-MSH–MC4R signaling pathway, we analyzed single-cell RNA-sequencing data from the PVN to identify neurons that express Alk. Interestingly, the data presented in Fig. 6 *A*–*D* show that Alk is not expressed in MC4R-expressing neurons, which otherwise coexpress thyrotropin-releasing hormone (TRH). Alk, on the other hand, is expressed in corticosterone-releasing hormone (CRH)–positive neurons. This result was confirmed by immunostaining analysis (Fig. 6*E*). These experiments show that MC4R and Alk are expressed in discrete populations of cells within the PVN, demonstrating that two distinct mechanisms that are also responsible for pigmentation operate within the PVN to control body weight.

Discussion

While it is now clear that Augα and Augβ bind specifically to the extracellular domains, stimulate tyrosine autophosphorylation of Alk and Ltk, and activate multiple intracellular signaling pathways (8, 9), the physiological roles of Augα and Augβ in mammals are essentially unknown. First insights into the physiological role of Augα and Augβ were described in genetic studies of zebrafish homologs of Augα and Augβ, revealing an important function of the Aug–Alk axis in control of neural crest–derived pigmentation during zebrafish development (12, 13). Mice deficient in Augα and Augβ individually or mice deficient in both molecules were generated to explore the

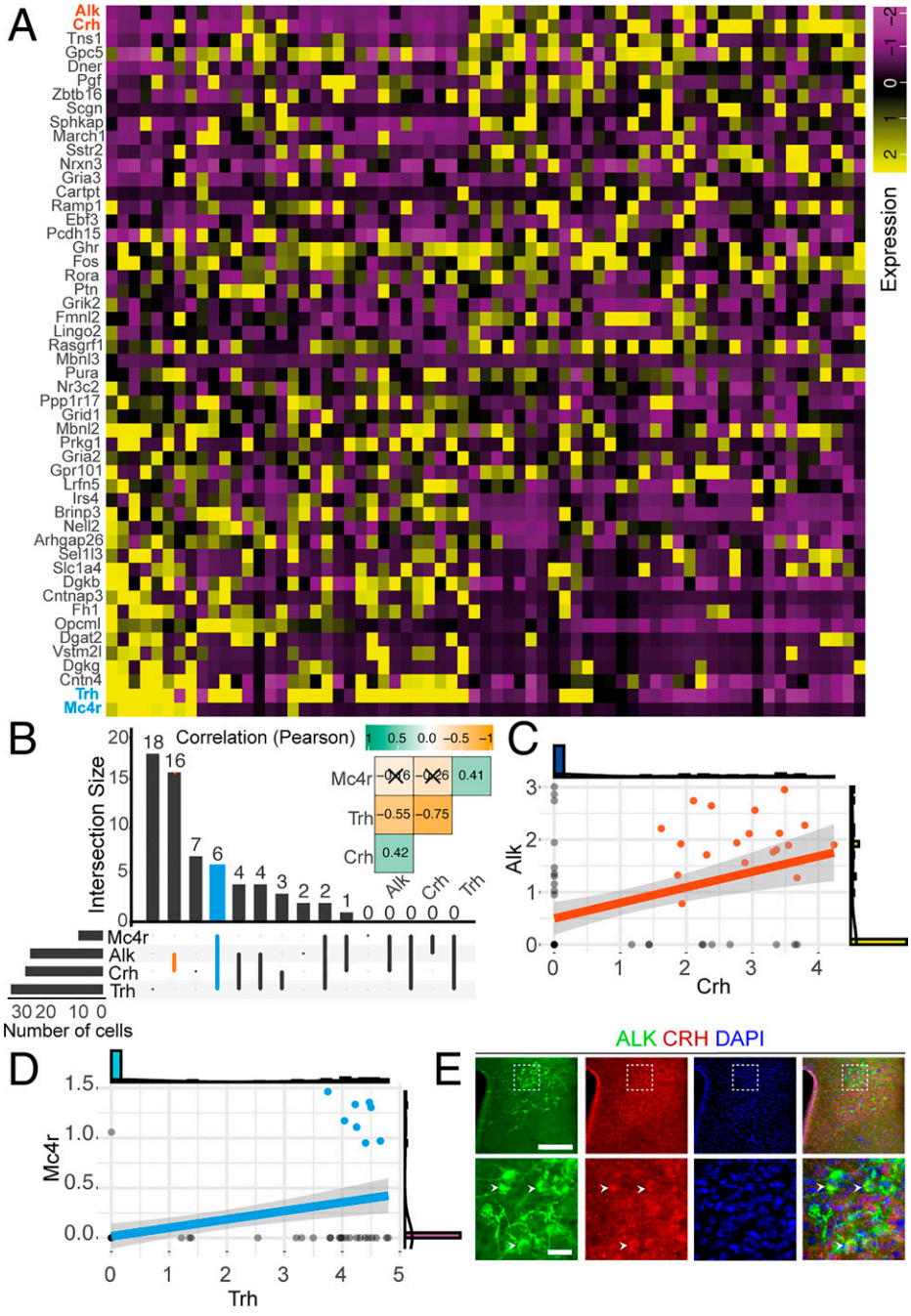

Fig. 6. Gene expression analysis of Alk- and MC4R-positive neurons in the PVN. (*A* and *B*) Heat map (*A*) and bar plot (*B*) showing differentially expressed genes from mouse hypothalamus RNA sequencing. (*C*) Scatter plot showing Alk and CRH correlation from the RNA-sequencing data. (*D*) Scatter plot showing MC4R and TRH correlation from the RNA-sequencing data. (*E*) Immunostaining showing colocalization of Alk (green) and CRH (red) in the PVN from P50 mice. *Bottom*, magnified image of dotted box from *Top*. (Scale bars, 40 μm and 200 μm, respectively.).

physiological roles of Alk and Ltk ligands. In this manuscript, we describe the role played by Augα in the modulation of brain functions. Experiments are presented demonstrating that Augα is expressed predominantly in AgRP neurons within the ARC in the hypothalamus and that starvation causes strong Augα expression in AgRP neurons, similar to other orexigenic molecules. It is also demonstrated that Augα-deficient mice are thin when either fed a normal diet or HFD. Upon 16 h of food deprivation, Augα-deficient mice displayed increased energy expenditure and RER, indicating failed energy-conserving mechanisms to cope with starvation. Furthermore, upon refeeding after fasting, Augα-knockout mice showed a slight decrease in food and water intake. Interestingly, Augα-deficient mice fed on standard chow showed a significant increase in energy expenditure, RERs, and activity without any significant change in food intake, indicating reduced efficiency of the orexigenic pathway to conserve energy. Consistently, Alk-deficient mice also show a similar phenotype of thinness attributed to high energy expenditure (22).

Augα-deficient mice showed reduced weight gain starting from the age of 3 to 4 wk in comparison to littermate controls, and weight differences continued to grow as the mice aged until 1 y, the last time point recorded. It is noteworthy that recent genome- and transcriptome-wide association studies identified Augα as a potential gene regulating obesity and basic metabolic rate (body mass index [BMI]) in humans. Moreover,

a transcriptome-wide association study identified 12 genes, including Fam150B (Augα), to be associated with childhood obesity. This study proposed Fam150B as a candidate gene for childhood BMI (26). Another consortium study in the United Kingdom on adults identified a single-nucleotide polymorphism near the Fam150B (Augα) locus to be associated with BMI and hereditable thinness in healthy thin ($n = 1{,}471$) versus severely obese ($n = 1{,}456$) individuals (27).

The demonstration that Augα-deficient mice are thinner than control mice is consistent with identification of an Estonian population cohort in which Alk was shown to be linked to thinness (22). Moreover, a short hairpin RNA screen in *Drosophila* and the phenotype of Alk-deficient mice also revealed thinness. Impaired Alk signaling in the PVN was implicated in increased WAT thermogenesis and as the cause for thin mice (22). Here, we demonstrate that Augα-expressing AgRP neurons project onto the Alk-expressing neurons in the PVN and that deletion of Augα leads to suppression of AgRP neuron projection into the PVN. Augα-expressing AgRP projections in the PVN are likely responsible for Alk activation as evident from reduced Alk activation in Augα-deficient mice. This result also provides a mechanistic link between Augα stimulation and thinness attributed to the deficiency of Alk expression in the PVN. Considering that AgRP neurons are part of the melanocortin system, that is, AgRP being a reverse agonist of MC4Rs, and both Alk and MC4R are expressed in the PVN, our study shows that the Augα–Alk signaling pathway is innate to but not overlapping with the central melanocortin system. Moreover, it also shows that two distinct mechanisms (α-MSH–MC4R regulating food intake and Augα–Alk regulating activity/energy expenditure) playing a central role in control of pigmentation act in concert in the hypothalamus to control body weight. Regarding the origin of AgRP projections to PVN Alk versus MC4R cells, it will be important to determine whether these segregated AgRP efferents to the PVN originate from the same cell bodies or from different parent cells. If they arise from the same cells, thereby representing collaterals, then the functional interplay between the melanocortin and Alk systems are more integrated in metabolism regulation than if they arise from nonoverlapping subpopulations of AgRP neurons. This knowledge could inform future therapeutic avenues.

In this manuscript, we also describe the initial characterization of the phenotype of Augα- and Augβ-deficient mice to pave the way for future mechanistic studies rather than provide a comprehensive analysis of the molecular mechanism underlying the phenotype of these mice. The higher physical activity of Augα-knockout mice during night and day could explain their increased energy expenditure linked to muscle contraction. Although the Augα-knockout mice seem to have a somewhat higher food intake, this increment may offset the increased caloric demand caused by increased muscle activity. Future experiments will determine whether the enhanced physical activity reflects behavioral alterations, for example, changes in eating behavior, anxiety/changes in day–night balance, and muscle-inherent modifications (e.g., changes in fiber composition, glycolytic versus oxidative fibers).

Finally, we conclude that the Augα–Alk signaling cascade represents a neuronal signaling pathway controlling metabolic processes that was co-opted to induce a variety of human cancers by aberrant expression of activated Alk mutants. Moreover, the recent elucidation of the three-dimensional structure of free and Aug-occupied ligand-binding region of Alk provides important new insights about how Augα and Augβ bind to Alk and Ltk and stimulate receptor dimerization and activation (11, 28, 29). It is noteworthy that a molecular mechanism established for ligand-induced Alk activation (11) is consistent with the mode of action of Augα described in our manuscript. Accordingly, Augα molecules produced in projections of AgRP neurons may act locally in close proximity to Alk-containing neurons in the PVN, resulting in their activation. The structural analyses reveal unique interactions with the cell membrane that together with reduced dimensionality enable efficient Augα-induced Alk activation. This mechanism is consistent with the locally Augα-induced Alk activation described in this report and is distinct from the common paradigm of how circulating hormones and growth factors (i.e., insulin, epidermal growth factor, or platelet-derived growth factor) activate their cognate receptors (1).

Materials and Methods

Detailed descriptions of the materials and methods used in this study are available in the *SI Appendix, Materials and Methods* (30–34).

Data Availability. All study data are included in the article and/or *SI Appendix*.

ACKNOWLEDGMENTS. We thank the N. Sestan laboratory in the Neuroscience Department at the Yale School of Medicine for supporting N.K. and using their facilities for imaging work. T.L.H. was supported by NIH grants AG052005, AG067329, and DK126447 and The Klarman Family Foundation. E.O.T. is supported by a scholarship from the Austrian Science Fund (FWF, DOC 33-B27). Single-cell RNA-sequencing data collection and processing were supported by the SECRET-CELLS and FOODFORLIFE ERC advanced grants (T.H.).

Author affiliations: [a]Department of Pharmacology, Yale School of Medicine, New Haven, CT 06520; [b]Department of Neuroscience, Yale School of Medicine, New Haven, CT 06520; [c]Department of Comparative Medicine, Yale School of Medicine, New Haven, CT 06520; [d]Department of Molecular Neurosciences, Medical University of Vienna, 1010 Vienna, Austria; and [e]Department of Neuroscience, Karolinska Institutet, 17177 Solna, Sweden

1. M. A. Lemmon, J. Schlessinger, Cell signaling by receptor tyrosine kinases. *Cell* **141**, 1117–1134 (2010).
2. S. W. Morris *et al.*, Fusion of a kinase gene, *ALK*, to a nucleolar protein gene, *NPM*, in non-Hodgkin's lymphoma. *Science* **263**, 1281–1284 (1994).
3. K. A. Suprenant, K. Dean, J. McKee, S. Hake, EMAP, an echinoderm microtubule-associated protein found in microtubule-ribosome complexes. *J. Cell Sci.* **104**, 445–450 (1993).
4. B. Hallberg, R. H. Palmer, Mechanistic insight into ALK receptor tyrosine kinase in human cancer biology. *Nat. Rev. Cancer* **13**, 685–700 (2013).
5. Q. Li, K. A. Suprenant, Molecular characterization of the 77-kDa echinoderm microtubule-associated protein. Homology to the beta-transducin family. *J. Biol. Chem.* **269**, 31777–31784 (1994).
6. C. M. Della Corte *et al.*, Role and targeting of anaplastic lymphoma kinase in cancer. *Mol. Cancer* **17**, 30 (2018).
7. H. Zhang *et al.*, Deorphanization of the human leukocyte tyrosine kinase (LTK) receptor by a signaling screen of the extracellular proteome. *Proc. Natl. Acad. Sci. U.S.A.* **111**, 15741–15745 (2014).
8. A. V. Reshetnyak *et al.*, Augmentor α and β (FAM150) are ligands of the receptor tyrosine kinases ALK and LTK: Hierarchy and specificity of ligand-receptor interactions. *Proc. Natl. Acad. Sci. U.S.A.* **112**, 15862–15867 (2015).
9. J. Guan *et al.*, FAM150A and FAM150B are activating ligands for anaplastic lymphoma kinase. *eLife* **4**, e09811 (2015).
10. A. V. Reshetnyak *et al.*, Identification of a biologically active fragment of ALK and LTK-Ligand 2 (augmentor-α). *Proc. Natl. Acad. Sci. U.S.A.* **115**, 8340–8345 (2018).
11. A. V. Reshetnyak *et al.*, Mechanism for the activation of the anaplastic lymphoma kinase receptor. *Nature* **600**, 153–157 (2021).
12. E. S. Mo, Q. Cheng, A. V. Reshetnyak, J. Schlessinger, S. Nicoli, Alk and Ltk ligands are essential for iridophore development in zebrafish mediated by the receptor tyrosine kinase Ltk. *Proc. Natl. Acad. Sci. U.S.A.* **114**, 12027–12032 (2017).
13. A. Fadeev *et al.*, ALKALs are in vivo ligands for ALK family receptor tyrosine kinases in the neural crest and derived cells. *Proc. Natl. Acad. Sci. U.S.A.* **115**, E630–E638 (2018).
14. E. Gropp *et al.*, Agouti-related peptide-expressing neurons are mandatory for feeding. *Nat. Neurosci.* **8**, 1289–1291 (2005).

15. S. Luquet, F. A. Perez, T. S. Hnasko, R. D. Palmiter, NPY/AgRP neurons are essential for feeding in adult mice but can be ablated in neonates. *Science* **310**, 683–685 (2005).
16. J. N. Campbell *et al.*, A molecular census of arcuate hypothalamus and median eminence cell types. *Nat. Neurosci.* **20**, 484–496 (2017).
17. F. E. Henry, K. Sugino, A. Tozer, T. Branco, S. M. Sternson, Cell type-specific transcriptomics of hypothalamic energy-sensing neuron responses to weight-loss. *eLife* **4**, e09800 (2015).
18. G. J. Morton, D. E. Cummings, D. G. Baskin, G. S. Barsh, M. W. Schwartz, Central nervous system control of food intake and body weight. *Nature* **443**, 289–295 (2006).
19. T. L. Horvath, The hardship of obesity: A soft-wired hypothalamus. *Nat. Neurosci.* **8**, 561–565 (2005).
20. K. E. Wortley *et al.*, Agouti-related protein-deficient mice display an age-related lean phenotype. *Cell Metab.* **2**, 421–427 (2005).
21. E. Roh, D. K. Song, M. S. Kim, Emerging role of the brain in the homeostatic regulation of energy and glucose metabolism. *Exp. Mol. Med.* **48**, e216 (2016).
22. M. Orthofer *et al.*, Identification of ALK in thinness. *Cell* **181**, 1246–1262 (2020).
23. H. Israeli *et al.*, Structure reveals the activation mechanism of the MC4 receptor to initiate satiation signaling. *Science* **372**, 808–814 (2021).
24. L. A. Lotta *et al.*, Human gain-of-function MC4R variants show signaling bias and protect against obesity. *Cell* **177**, 597–607 (2019).
25. A. C. P. da Fonseca *et al.*, Identification of the *MC4R* start lost mutation in a morbidly obese Brazilian patient. *Diabetes Metab. Syndr. Obes.* **12**, 257–266 (2019).
26. S. Yao *et al.*, Transcriptome-wide association study identifies multiple genes associated with childhood body mass index. *Int. J. Obes.* **45**, 1105–1113 (2021).
27. F. Riveros-McKay *et al.*; Understanding Society Scientific Group, Genetic architecture of human thinness compared to severe obesity. *PLoS Genet.* **15**, e1007603 (2019).
28. T. Li *et al.*, Structural basis for ligand reception by anaplastic lymphoma kinase. *Nature* **600**, 148–152 (2021).
29. S. De Munck *et al.*, Structural basis of cytokine-mediated activation of ALK family receptors. *Nature* **600**, 143–147 (2021).
30. N. Sestan, S. Artavanis-Tsakonas, P. Rakic, Contact-dependent inhibition of cortical neurite growth mediated by notch signaling. *Science* **286**, 741–746 (1999).
31. E. S. Lein *et al.*, Genome-wide atlas of gene expression in the adult mouse brain. *Nature* **445**, 168–176 (2007).
32. R. A. Romanov *et al.*, Molecular design of hypothalamus development. *Nature* **582**, 246–252 (2020).
33. Y. Hao *et al.*, Integrated analysis of multimodal single-cell data. *Cell* **184**, 3573–3587 (2021).
34. J. R. Conway, A. Lex, N. Gehlenborg, UpSetR: An R package for the visualization of intersecting sets and their properties. *Bioinformatics* **33**, 2938–2940 (2017).